Supporting Information

Gournas et al. 10.1073/pnas.1719462115

SI Materials and Methods

Yeast Strains and Growth Conditions. The yeast strains used in this study (Table S1) derive from strain Σ1278b. The *rsp5 (npi1-1)* strain is a viable *rsp5* mutant where a Ty element inserted in the upstream control region of the gene results in severely reduced expression of *RSP5* (1). Cells were grown at 29 °C on a minimal buffered medium, pH 6.1 (2), with Gal (3%), Raf (3%), or Glu (3%) as the carbon source. The nitrogen sources present in the growth medium were, as indicated, Am in the form of $(NH_4)_2SO_4$ (10 mM), Pro (10 mM), glutamine (10 mM), or Arg (5 mM). Difco YNB was used in the experiments shown in Fig. 3*A*, as we noticed that the Pil1(4A) is not epistatic to the deletion of *NCE102* in our buffered medium. The final concentrations of substances added to solid or liquid media were Arg (5 mM), lysine (5 mM), Myr (10 μM), AbA (1 μg/mL), and Rap (200 ng/mL). The *CAN1-GFP* and *GAP1-GFP* genes were expressed under the control of the *GAL* promoter or their native promoter. When cells were grown on Gal medium, pGAL1-driven expression was repressed by the addition of 3% Glu, 0.5 or 1.5 h before treatment, cell filtration, or microscopic observation of the cells. The tagged versions of *SUR7*, *PIL1*, and *NCE102* were expressed under their respective native promoters. Comparative analysis of growth in liquid cultures was performed by growing cells in a 24-well Greiner microplate incubator coupled to a SYNERGY multimode reader (BioTek Instruments). For epifluorescence and confocal microscopy, cells derived from exponentially growing early logarithmic phase liquid cultures or from cultures that had reached the stationary phase of growth were laid on a thin layer of 1% agarose (occasionally supplemented with the same substances/conditions used to treat the culture) and observed at room temperature by epifluorescence microscopy or at 29 °C by confocal microscopy.

Plasmids Used in This Study. The plasmids used in this study are listed in Table S2. Plasmids isolated during this work were constructed by in vivo recombination in yeast. Each plasmid was purified by cloning into *Escherichia coli* and checked by sequencing.

Wide-Field Fluorescence Microscopy. The endocytosis of Can1-GFP and Gap1-GFP was evaluated by observation with an Eclipse 80i (Nikon) epifluorescence microscope equipped with a 100× differential interference contrast, NA 1.40 Plan-Apochromat objective (Nikon), and appropriate fluorescence light filter sets. Images were captured with a DS-Qi1Mc-U3 (Nikon) digital camera and NIS-Elements 4.3 acquisition software (Nikon). Labeling of cell vacuoles was performed for 15 min in liquid medium with 250 μM CellTracker Blue CMAC dye (Life Technologies). Cells were washed and resuspended in CMAC-free medium before imaging. Images were then autocorrected for optimal brightness and contrast, cropped, merged using FIJI software (NIH) (3), and annotated with Photoshop CS5 (Adobe Systems).

Quantification of Wide-Field Fluorescence Microscopy. The fluorescence intensity of Can1-GFP was quantified with FIJI software (3), as previously reported (4). In brief, two ellipses, one outlining the cell and another on the inside, excluding the PM, were drawn manually ($n > 90$ cells). In the corresponding figures, PM/-internal mean pixel-intensity ratios for each cell population are presented in box-and-whisker plots.

Confocal Microscopy. Images were acquired with a Zeiss LSM710 microscope equipped with Airyscan and a 100× differential interference contrast, NA 1.46 Alpha-Plan-Apochromat objective, with ZEN 2.1 SP2 software. GFP fluorescence was excited with the 488-nm line of the argon laser; mRFP, mCherry, and mKate2 fluorescence were excited with a 594-nm solid-state laser; mtagBFP2 fluorescence was excited with a 405-nm diode laser, and appropriate filters and beam splitters were used. Airyscan processing was performed with the ZEN software, using the default settings. The final pixel size was 38.5 nm. The same laser intensities and other settings of the confocal microscope were used for all image acquisition. Images were then autocorrected for optimal brightness and contrast, cropped, merged using FIJI software (3), and annotated with Photoshop CS5 (Adobe Systems). In each figure only a few cells representative of the whole cell population, observed in at least two independent biological replicate experiments, are shown.

Quantification of Protein Clustering in EMCs and EMC Parameters. Confocal microscopy images were analyzed with a custom-made FIJI macro. The image of the EMC marker (Pil1) was processed first to create a mask of the EMCs. For each experiment, the better of the two following processing methods was used. (*i*) A 3 × 3 median filter (despeckle function) was applied, the ImageJ default thresholding method was applied, and then overlapping EMCs were separated using the watershed function. (*ii*) Alternatively, before default thresholding, the sharpen function and a Fourier space high-pass filter were applied, followed by the despeckle and dilate functions. After the EMC mask was obtained, the outlines of the focused cell surfaces were manually drawn with the ellipse tool, with the Can1, Gap1, or Nce102 image as a support for the user. The intensities of the channels of interest were measured both inside the complete cell outlines and in the EMC-positive area. The median of the fluorescence intensity in the whole image was used as a measure of the background. The tendency of the protein of interest to localize to the EMCs was measured as the ratio of the background-corrected mean intensity per pixel of the EMC area to that of the area delimited by the whole-cell outline and excluding the EMC area. The EMC density was calculated as the number of EMC-positive objects per total area of the outlined region. The EMC/total surface area ratio was defined as the ratio of the area of EMC-positive objects to the area of the outlined region. The Pearson's correlation coefficient was determined using a custom-made macro based on the coloc2 plugin of FIJI. Note that due to the much higher number of EMCs and the fluorescence intensity of Pil1-mCherry in late stationary phase, our custom-made script sometimes tended to recognize closely localized EMCs as one EMC. This leads to a slight underestimation of both the EMC clustering of Can1 (compared with the Pearson's correlation coefficient) and the number of EMCs during late stationary phase and also to a slight overestimation of the percentage of the PM covered by EMCs. All parameters were calculated from at least two independent biological replicates for each condition. The values for single cells are presented in box-and-whisker plots. After confirming statistically that the two independent biological replicates gave statistically nonsignificant differences in mean values, the values of the two independent experiments were merged.

Statistical Analysis of Quantifications. Prism software, ANOVA with the nonparametric Kruskal–Wallis test, and Dunn's

multiple-comparison post hoc analyses were used to assess the significance of the value differences of all measurements.

FRAP. One or two tangential sections per cell of a membrane surface of fixed size (13 pixels) were photobleached with 100%-intensity pulses of the 488-nm line of the argon laser coupled to the LSM710 microscope. Confocal microscopy images, produced with the Airyscan module, were used to monitor the recovery of fluorescence by acquiring either 10-s intervals up to 600 s or 1- to 2-min intervals up to 36 min, depending on the kinetics of recovery. Cells were kept focused with Definite Focus (Zeiss). The intensity of fluorescence in the region of interest (EMC or non-EMC) was measured with ImageJ, background-subtracted and corrected for voluntary and nonvoluntary photobleaching, and expressed as a percentage of the fluorescence intensity before photobleaching. Values from at least eight independent experiments were introduced in GraphPad Prism and analyzed with the one-phase association equation, calculating the best fit values for the half-time (ln2/K) and the 99% CIs. Additionally, an extra-sum-of-squares F test was performed with GraphPad Prism to calculate the probability (F-pvalue) that the calculated K values do not differ.

Protein Extracts. For immunoblot analyses, crude cell extracts were prepared and analyzed by SDS/PAGE as previously described (1). Membrane-enriched extracts were prepared as in ref. 5. Briefly, cells from 500 ml cultures with an OD of 0.25 were filtered and frozen at −80 °C. The cells were washed with 5 mL TNE buffer [50 mM Tris·HCl (pH 7.4), 150 mM NaCl, 5 mM EDTA], resuspended in 2 mL TNE-I buffer [TNE supplemented with protease inhibitor mixture (Sigma) and 1 mM PMSF], and lysed by adding 800 μL of glass beads, followed by vortexing for 40 min at 4 °C. Cell debris was removed by a 4-min centrifugation at 500 × g and 4 °C, the supernatant was transferred to another tube, and crude membranes were pelleted by centrifugation at 16,100 × g for 90 min at 4 °C. Extracts of membrane-enriched preparations were resuspended in 100 μL TNE-I buffer. Protein concentrations were determined by Bradford's method.

Determination of Can1 detergent resistance was performed as in ref. 6. Briefly, aliquots of protein extracts from membrane-enriched preparations, corresponding to 30 μg protein, were treated at room temperature for 30 min with increasing concentrations of Triton X-100 (0–0.8%) in a final volume of 60 μL TNE-I. The nonsolubilized material was pelleted by centrifugation (16,100 × g at 4 °C for 30 min) and washed with 100 μL TNE-I buffer containing the corresponding concentration of Triton X-100. Pellets were resuspended in 30 μL sample buffer, dissociated at 90 °C for 2 min, resolved by SDS/PAGE, immunoblotted with anti-GFP antibody, and subsequently stripped and immunoblotted with anti-Gap1 and anti-Pma1 antibodies.

Western Blotting and Quantification of Signals. Proteins resolved by SDS/PAGE were transferred to a nitrocellulose membrane (Protran, Perkin-Elmer) and probed with a mouse monoclonal anti-GFP (Roche) or with rabbit polyclonal anti-Gap1 or anti-Pma1 (7). Primary antibodies were detected by enhanced chemiluminescence (Roche) after treatment with HRP-conjugated anti-mouse or anti-rabbit IgG secondary antibody (Sigma). Signals were detected with CL-Xposure film (Thermo Scientific). Films were scanned and annotated with Photoshop CS5. Signals from three biological replicate experiments were quantified from non-saturated exposures using ImageJ and were expressed as a percentage of the control (OD = 0.1 or nontreated) signal. Statistical analyses of the significance of differences were performed with GraphPad Prism using the repeated-measures two-way ANOVA analyses for matched values spread across a row, coupled to Sidak's multiple-comparisons test.

Permease Activity Assays and Determination of Can1 Kinetic Characteristics. Permease transport activities were determined by measuring, with a β-counter, accumulated counts showing the initial rate of [^{14}C]-labeled amino acid uptake (20, 40, and 60 s) (Perkin-Elmer), corrected for protein concentration, as previously described (7). Uptake rates are expressed in nanomoles per milligram of protein per unit of time and are reported as means ± SD (n = 2–3). At least eight substrate concentrations, ranging from 1 to 80 μM, were used to determine the apparent K_m and the V_m for [^{14}C]Arg uptake. The values gave a good fit with single-site Michaelis–Menten kinetics. Data were analyzed with GraphPad Prism version 5.0, calculating the K_m and V_m values as well as their 99% CIs. Additionally, an extra-sum-of-squares F test was performed with GraphPad Prism to calculate the F-pvalue.

1. Hein C, Springael J-Y, Volland C, Haguenauer-Tsapis R, André B (1995) NPl1, an essential yeast gene involved in induced degradation of Gap1 and Fur4 permeases, encodes the Rsp5 ubiquitin-protein ligase. *Mol Microbiol* 18:77–87.
2. Jacobs P, Jauniaux J-C, Grenson M (1980) A cis-dominant regulatory mutation linked to the argB-argC gene cluster in Saccharomyces cerevisiae. *J Mol Biol* 139:691–704.
3. Schindelin J, et al. (2012) Fiji: An open-source platform for biological-image analysis. *Nat Methods* 9:676–682.
4. Gournas C, et al. (2017) Transition of yeast Can1 transporter to the inward-facing state unveils an α-arrestin target sequence promoting its ubiquitylation and endocytosis. *Mol Biol Cell* 28:2819–2832.
5. Grossmann G, Opekarová M, Malinsky J, Weig-Meckl I, Tanner W (2007) Membrane potential governs lateral segregation of plasma membrane proteins and lipids in yeast. *EMBO J* 26:1–8.
6. Grossmann G, et al. (2008) Plasma membrane microdomains regulate turnover of transport proteins in yeast. *J Cell Biol* 183:1075–1088.
7. Ghaddar K, et al. (2014) Converting the yeast arginine can1 permease to a lysine permease. *J Biol Chem* 289:7232–7246.

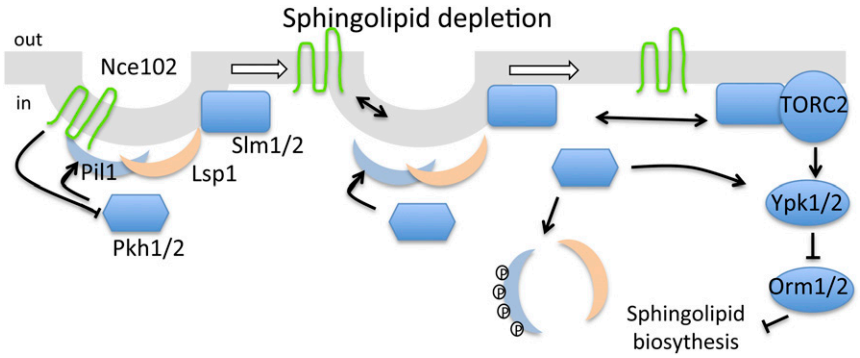

Fig. S1. Organization of EMCs. Schematic representation of EMCs and their role in controlling SL biosynthesis. Upon SL depletion the eisosome-resident Pkh1/2 kinases phosphorylate Pil1, causing eisosome disassembly followed by relocalization of the Slm1/2 proteins to the MCT to activate the Ypk1 kinase via TORC2-dependent phosphorylation. Activated Ypk1 then phospho-inhibits the Orm1/2 proteins, negative regulators of serine palmitoyl-transferase, which catalyze the first step in SL biosynthesis.

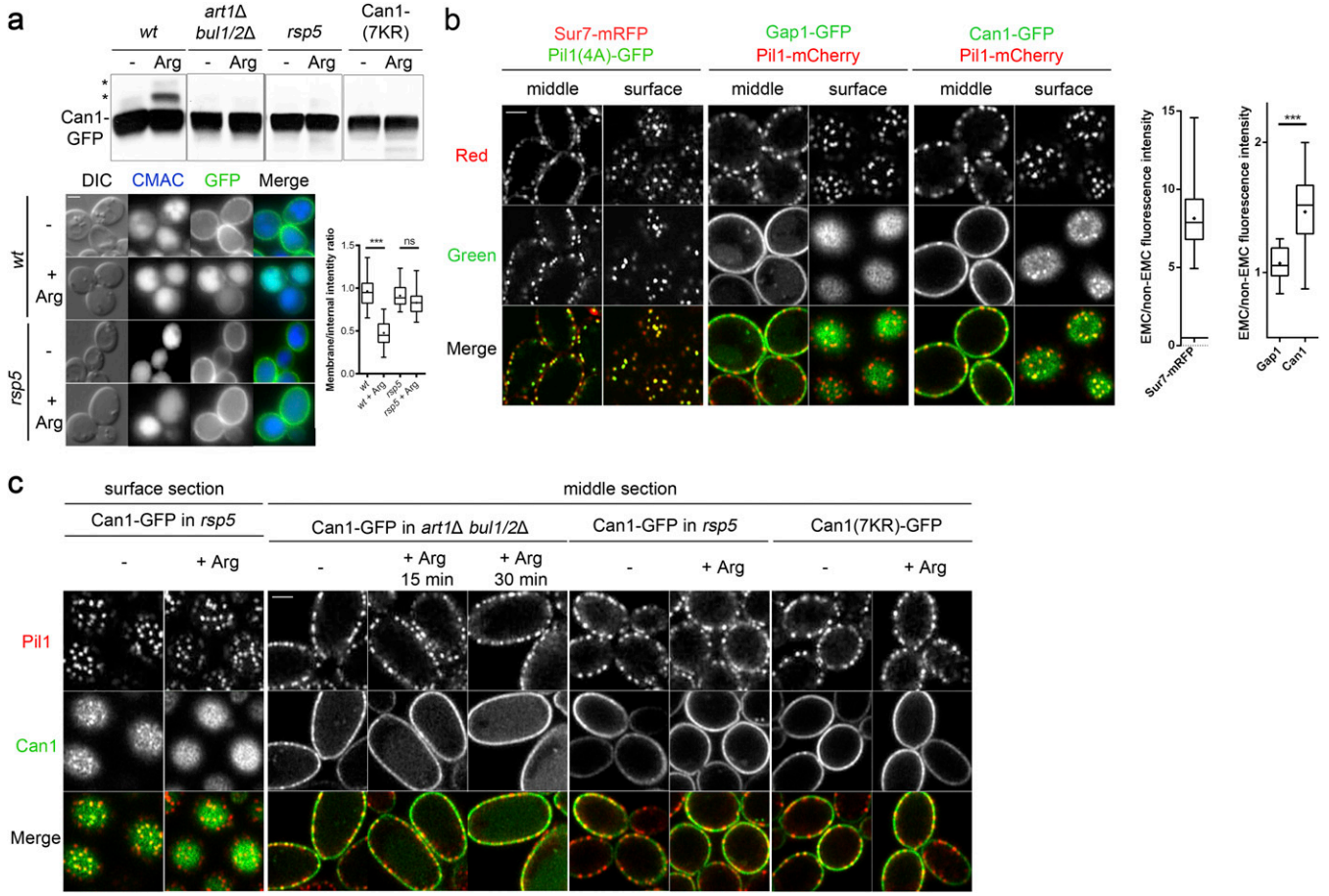

Fig. S2. Related to Fig. 1. (*A*, *Upper*) WT, *rsp5*, and *art1*Δ *bul1/2*Δ strains (*gap1*Δ *can1*Δ) expressing either Can1-GFP or Can1(7KR)-GFP from the *GAL1* promoter, were grown in Gal Pro medium. Glu was added for 90 min, and then the cells were treated or not for 30 min with Arg (5 mM). Total protein extracts were probed with anti-GFP. Asterisks indicate Ub-Can1-GFP conjugates. (*Lower*, *Left*) Strains (*gap1*Δ *can1*Δ) expressing Can1-GFP were grown on Gal Pro medium. Can1-GFP expression under the control of the *GAL1* promoter was repressed by the addition of 3% Glu for 1.5 h. Arg (5 mM) was then added for 3 h. After CMAC staining, the cells were observed by epifluorescence microscopy. (*Lower Right*) Quantifications: PM/intracellular GFP fluorescence intensity ratios are plotted ($n = 78$ cells). Representation is as in Fig. 1*B*. (*B*, *Left*) The method used to quantify the fluorescence intensity of tagged membrane proteins in EMCs. Cells expressing GFP-, mRFP-, or mCherry-tagged eisosomal proteins and Can1-GFP or Gap1-GFP were observed by confocal microscopy coupled to Airyscan detection. Surface and middle sections were acquired. After Airyscan processing, the cells were analyzed with a custom-made script for FIJI which automatically detects eisosomes and calculates the mean intensity of fluorescence inside and outside the EMCs (see also *Materials and Methods*). (*Right*) Quantifications ($n =$ 23–47) are presented as in Fig. 1*B*. (*C*) Arg addition does not affect the assembly of eisosomes. Shown are middle sections of the cells shown in Fig. 1*B*. ***$P <$ 0.001; ns, nonsignificant, $P > 0.05$. (Scale bar: 2 μm.).

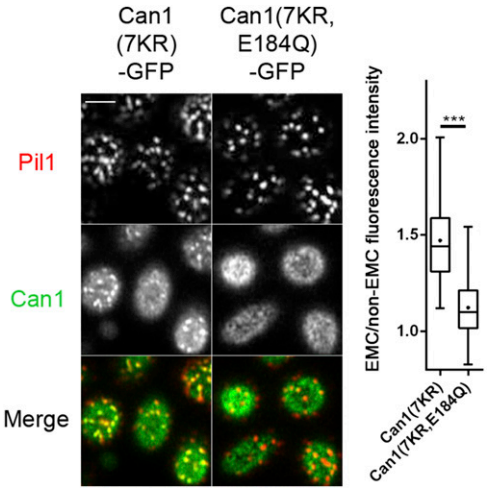

Fig. S3. Related to Fig. 2. The Can1(7KR,E184Q)-GFP mutant does not cluster in the MCC. Shown are surface section confocal microscopy images of a *gap1*Δ *can1*Δ *PIL1-mCherry* strain expressing Can1(7KR)-GFP or Can1(7KR,E184Q)-GFP. Conditions and quantifications ($n = 34–92$) are as in Fig. 1*B*. ***$P < 0.001$. (Scale bar: 2 μm.)

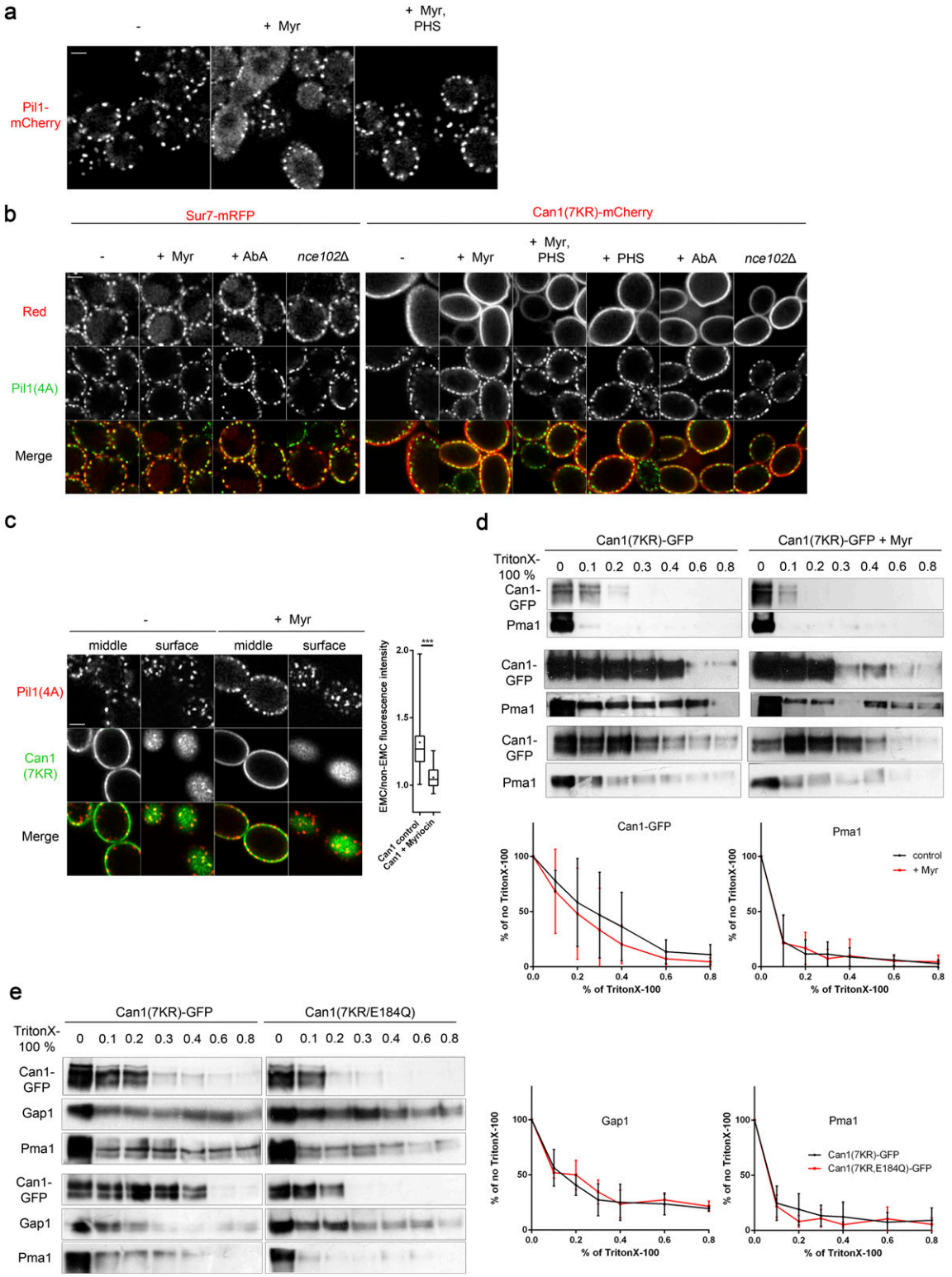

Fig. S4. Related to Fig. 3. Can1 EMC localization requires SLs. (*A*) Shown are middle section confocal microscopy images of Pil1-mCherry–expressing cells treated or not with 10 μM Myr, in the presence or absence of PHS for 90 min. (*B*) Inhibiting SL biosynthesis (10 μM Myr or 1 μg/mL AbA for 90 min) does not affect Pil1(4A)-GFP–containing eisosomes. Shown are middle section confocal microscopy images of the cells shown in Fig. 3*A*. (*C*) After treatment with 10 μM Myr for 90 min, Can1(7KR)-GFP no longer clusters in Pil1(4A)-MARS–containing eisosomes under the conditions used in the experiment shown in Fig. S3*D*. Shown are middle and surface confocal microscopy images of a *gap1*Δ *can1*Δ *PIL1(4A)-MARS* strain expressing Can1(7KR)-GFP, treated or not with 10 μM Myr for 90 min. Quantifications ($n = 28–39$) are as in Fig. 1*B*. (*D*) Detergent resistance of Can1(7KR)-GFP. A *can1*Δ *gap1*Δ strain expressing Pil1(4A)-MARS as the sole Pil1 and Can1(7KR)-GFP under the control of the *GAL1* promoter was grown on Gal Pro medium. After Glu addition for 1.5 h, cells were treated or not with 10 μM Myr for 90 min. Thirty-microgram aliquots of membrane-enriched protein extracts were treated with increasing concentrations of Triton X-100. Following centrifugation and washing, the detergent-resistant insoluble pellet was resuspended in sample buffer and blotted with anti-GFP antibody. Subsequently, the

Legend continued on following page

membranes were stripped and immunoblotted with anti-Pma1. Three independent biological replicates were performed and quantified, as in Fig. 3*D*, for the percentage of Can1-GFP and Pma1 signals in comparison with the extracts treated in the absence of Triton X-100. (*E*, *Left*) Two additional biological replicates of the detergent resistance of Can1(7KR) and Can1(7KR,E184Q), performed and analyzed as in Fig. 3*D*. (*Right*) Quantifications, as in Fig. 3*D*, of the signals of Gap1 and Pma1. ***$P < 0.001$. (Scale bar: 2 μm.)

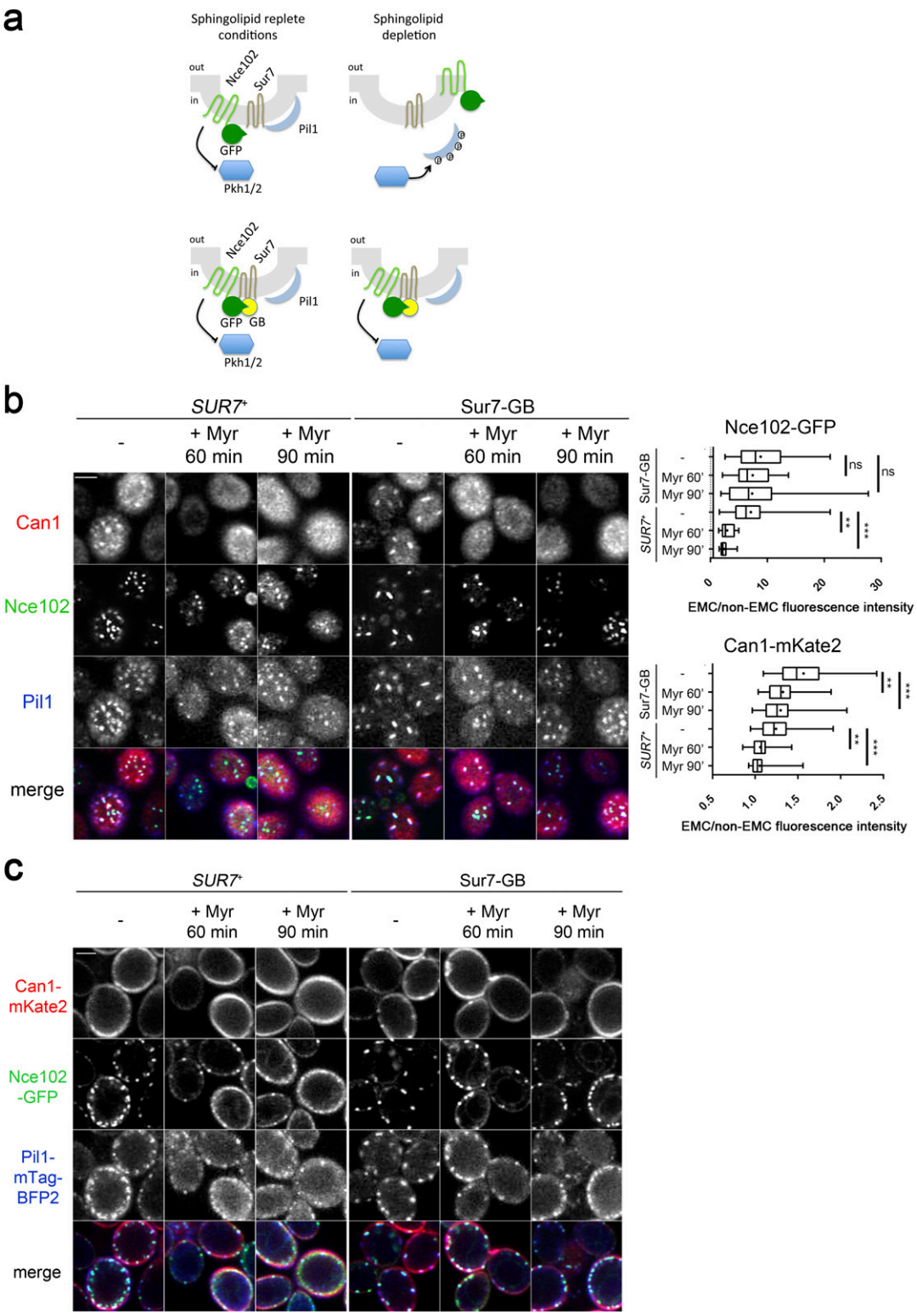

Fig. S5. Related to Fig. 3. Nce102 is not essential for EMC clustering of Can1. (*A*) Schematic representation of the principle. (*Upper*) In WT cells SL depletion leads to Nce102 exit from the EMCs, relieving its inhibitory effect on the Pkh1/2 kinases present under SL-replete conditions. Phosphorylation of Pil1 leads to eisosome disassembly. (*Lower*) In the presence of Sur7-GB, Nce102-GFP is tethered in the EMCs even upon SL depletion. Consequently, the Pkh1/2 kinases remain inhibited, and the eisosomes do not disassemble upon SL depletion. (*B* and *C*, *Left*) Surface (*B*) and middle (*C*) section confocal microscopy of *SUR7-GB* and *SUR7* strains (*gap1*Δ *can1*Δ) expressing Pil1-mTagBFP2, Nce102-GFP, and Can1(7KR)-mKate2, treated or not with 10 μM Myr for 60 or 90 min. (*B*, *Right*) Quantifications ($n = 22–63$) are as in Fig. 1*B*. In *C*, Sur7-GB– and Nce102-GFP–expressing cells, Pil1-mtagBFP2-labeled eisosomes are not affected by up to 90-min treatment with 10 μM Myr. ***$P < 0.001$; **$P < 0.01$; ns, nonsignificant, $P > 0.05$. (Scale bar: 2 μm.)

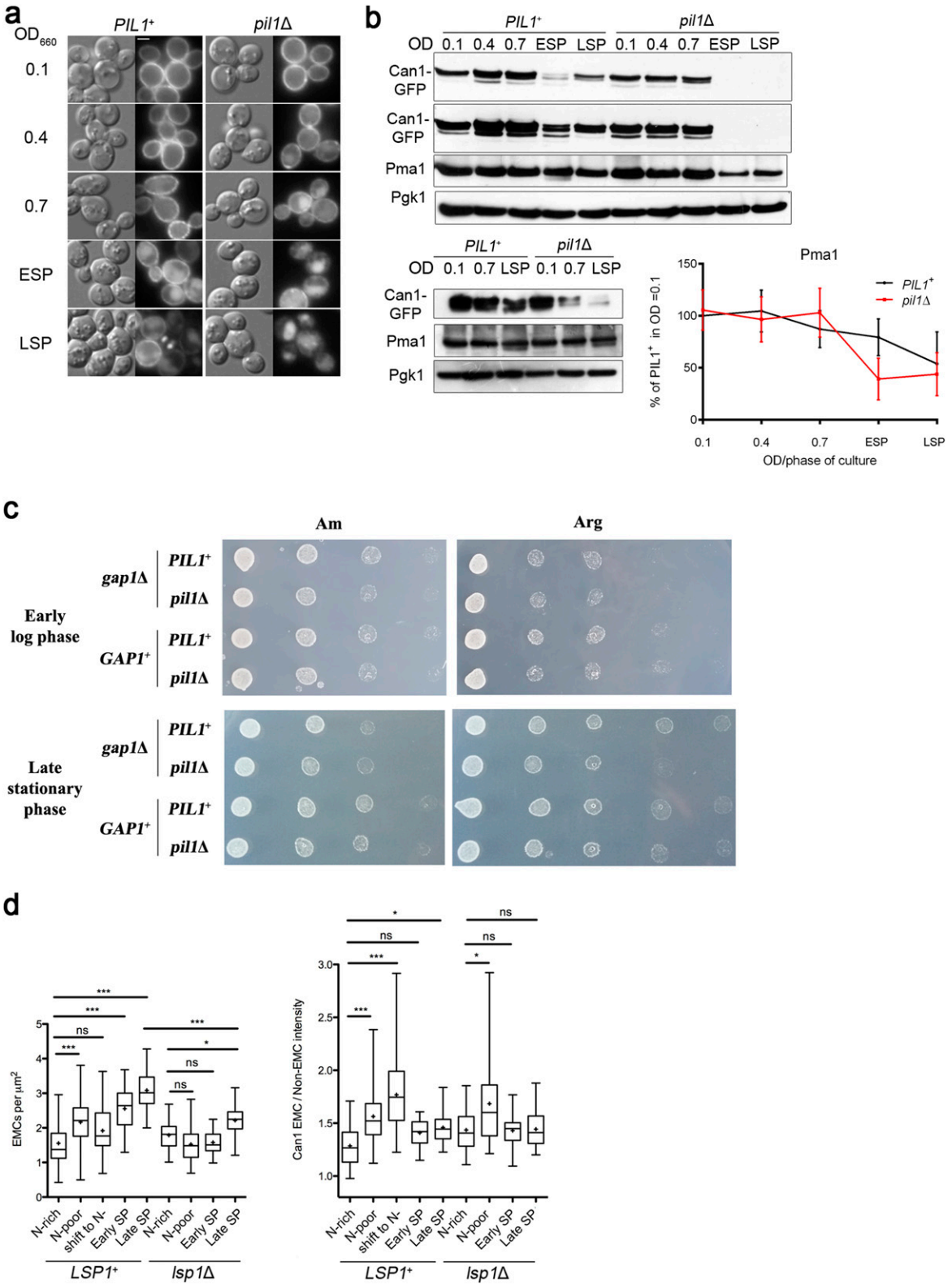

Fig. S6. Related to Fig. 5. (*A*) Epifluorescence microscopy of *PIL1* and *pil1*Δ cells (*gap1*Δ *can1*Δ) expressing Can1-GFP and grown in glutamine plus Am at different ODs or having reached (ESP) or having remained for 12 h in (LSP) the stationary phase. (*B*) Two additional biological replicates and quantification of the Pma1 signals of the experiment shown in Fig. 5*D*. Analysis and quantifications are as in Fig. 5*D*. (*C*) Spot dilution tests of *PIL1* and *pil1*Δ cells, containing or not the *gap1*Δ mutation, from early logarithmic phase cultures and cultures having remained in the stationary phase for 12 h. (*D*) Quantifications of the number of EMCs/μm^2 and Can1 EMC/non-EMC fluorescence intensity ratio for the results presented in Fig. 5*F*. For details see *Materials and Methods*. ***$P <$ 0.001; *$P < 0.05$; ns, nonsignificant, $P > 0.05$.

Table S1. *S. cerevisiae* strains used in this study

Strain	Genotype	Ref. or source
23344c	*ura3*	Laboratory collection
EK008	*gap1Δ ura3*	Laboratory collection
35283a	*can1Δ gap1Δ npi1-1(rsp5) ura3*	(1)
ES029	*can1Δ gap1Δ ura3*	(1)
ES032	*can1Δ ura3*	(1)
CG052	*art1Δ bul1Δ bul2Δ can1Δ gap1Δ ura3*	(1)
MYC013	*pil1Δ gap1Δ ura3*	This study
CG050	*pil1Δ can1Δ gap1Δ ura3*	This study
CG056	*pil1Δ ura3*	This study
SG001	*PIL1(4A)-GFP::URA3 pil1Δ SUR7-mRFP-LEU2 leu2Δ can1Δ gap1Δ ura3*	This study
SG023	*PIL1(4A)-mRFPmars can1Δ gap1Δ ura3*	This study
SG035	*PIL1-mCherry can1Δ gap1Δ ura3*	This study
SG041	*PIL1-mCherry art1Δ bul1Δ bul2Δ can1Δ gap1Δ ura3*	This study
SG043	*PIL1-mCherry can1Δ gap1Δ npi1-1(rsp5) ura3*	This study
SG047	*SUR7-GB can1Δ gap1Δ ura3*	This study
SG057	*SUR7-GB pil1Δ can1Δ gap1Δ ura3*	This study
SG067	*SUR7-GB PIL1-mCherry can1Δ gap1Δ ura3*	This study
SG081	*SUR7-GB can1Δ gap1Δ ura3 leu2Δ*	This study
CG071	*PIL1-mCherry art1Δ bul1Δ bul2Δ gap1Δ ura3*	This study
CG098	*PIL1(4A)-GFP::URA3 pil1Δ leu2Δ can1Δ gap1Δ ura3*	This study
CG100	*PIL1(4A)-GFP::URA3 pil1Δ nce102Δ leu2Δ can1Δ gap1Δ ura3*	This study
CG108	*SUR7-mRFP-LEU2 PIL1(4A)-GFP::URA3 pil1Δ leu2Δ can1Δ gap1Δ ura3*	This study
CG110	*SUR7-mRFP-LEU2 PIL1(4A)-GFP::URA3 pil1Δ nce102Δ leu2Δ can1Δ gap1Δ ura3*	This study
CG116	*lsp1Δ PIL1-mCherry can1Δ gap1Δ ura3*	This study
CG092	*PIL1-BFP2 SUR7-GB can1Δ gap1Δ ura3 leu2Δ*	This study
CG102	*PIL1-BFP2 can1Δ gap1Δ ura3 leu2Δ*	This study
CG136	*nce102Δ PIL1-BFP2 SUR7-GB can1Δ gap1Δ ura3 leu2Δ*	This study
CG138	*nce102Δ PIL1-BFP2 can1Δ gap1Δ ura3 leu2Δ*	This study

1. Gournas C, et al. (2017) Transition of yeast Can1 transporter to the inward-facing state unveils an α-arrestin target sequence promoting its ubiquitylation and endocytosis. *Mol Biol Cell* 28:2819–2832.

Table S2. Plasmids used in this study

Plasmid	Description	Ref. or source
pFL038	CEN-ARS (URA3)	(1)
pJOD010	CEN-ARS GAL1-GAP1-GFP (URA3)	(2)
pKG036	CEN-ARS CAN1-GFP (URA3)	(3)
pCJ563	CEN-ARS GAL1-CAN1-GFP (URA3)	(3)
pCJ560	CEN-ARS GAL1-CAN1(E184Q)-GFP (URA3)	(4)
pCJ565	CEN-ARS GAL1-CAN1(T180R)-GFP (URA3)	(4)
pCJ574	CEN-ARS GAL1-CAN1(E184A)-GFP (URA3)	(4)
pCG025	CEN-ARS GAL1-CAN1(ELK89-AAA)-GFP (URA3)	(4)
pCG030	CEN-ARS GAL1-CAN1(S176N-T456S)-GFP (URA3)	(4)
pCG031	CEN-ARS GAL1-CAN1(S176N-E184Q)-GFP (URA3)	(4)
pCG032	CEN-ARS GAL1-CAN1(S176N)-GFP (URA3)	(4)
pCG065	CEN-ARS GAL1-CAN1(T180R/E184Q)-GFP (URA3)	(4)
pCG080	CEN-ARS GAL1-CAN1(K5R/K13R/K42R/K45R/K47R/K85R/K89R)-GFP (URA3)	(4)
pCG108	CEN-ARS GAL1-CAN1(K5R/K13R/K42R/K45R/K47R/K85R/K89R)-mCherry (LEU2)	(4)
pRS306-pil1_GFP Nr::6	PIL1(4A)-GFP (URA3)	(5)
pCG106	CEN-ARS GAL1-CAN1(K5R/K13R/K42R/K45R/K47R/K85R/K89R/E184Q)-GFP (URA3)	This study
pCG114	CEN-ARS GAL1-CAN1(K5R/K13R/K42R/K45R/K47R/K85R/K89R/E184Q)-mKate2 (LEU2)	This study
pCG118	CEN-ARS-NCE102-GFP (URA3)	This study

1. Bonneaud N, et al. (1991) A family of low and high copy replicative, integrative and single-stranded S. cerevisiae/E. coli shuttle vectors. *Yeast* 7:609–615.
2. Nikko E, Marini AM, André B (2003) Permease recycling and ubiquitination status reveal a particular role for Bro1 in the multivesicular body pathway. *J Biol Chem* 278:50732–50743.
3. Ghaddar K, et al. (2014) Converting the yeast arginine can1 permease to a lysine permease. *J Biol Chem* 289:7232–7246.
4. Gournas C, et al. (2017) Transition of yeast Can1 transporter to the inward-facing state unveils an α-arrestin target sequence promoting its ubiquitylation and endocytosis. *Mol Biol Cell* 28:2819–2832.
5. Walther TC, et al. (2007) Pkh-kinases control eisosome assembly and organization. *EMBO J* 26:4946–4955.

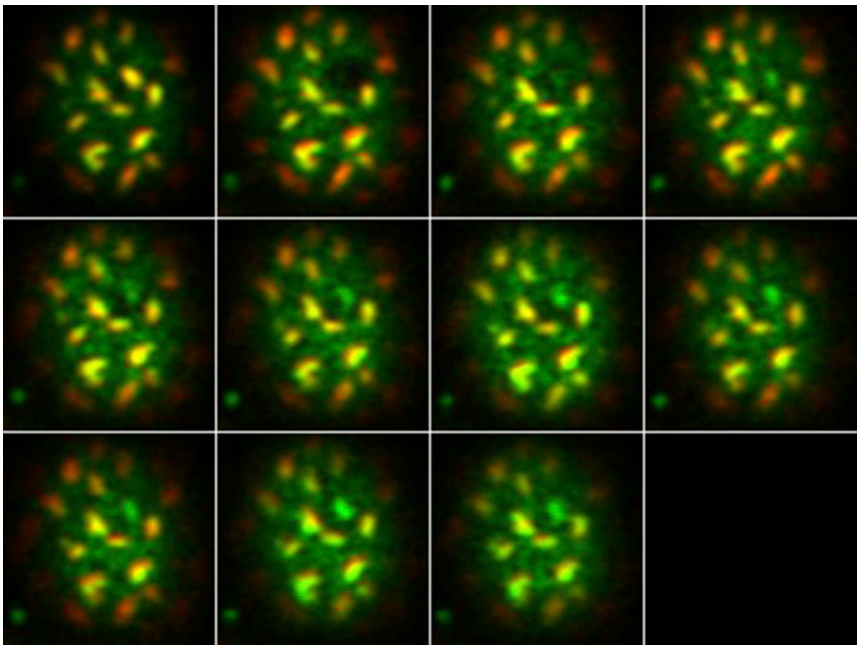

Movie S1. Representative FRAP analysis of Can1(7KR)-GFP in the EMC in the absence of substrate. Frames correspond to 2-min intervals, up to 18 min after photobleaching. Related to Fig. 1*C*.

Movie S1

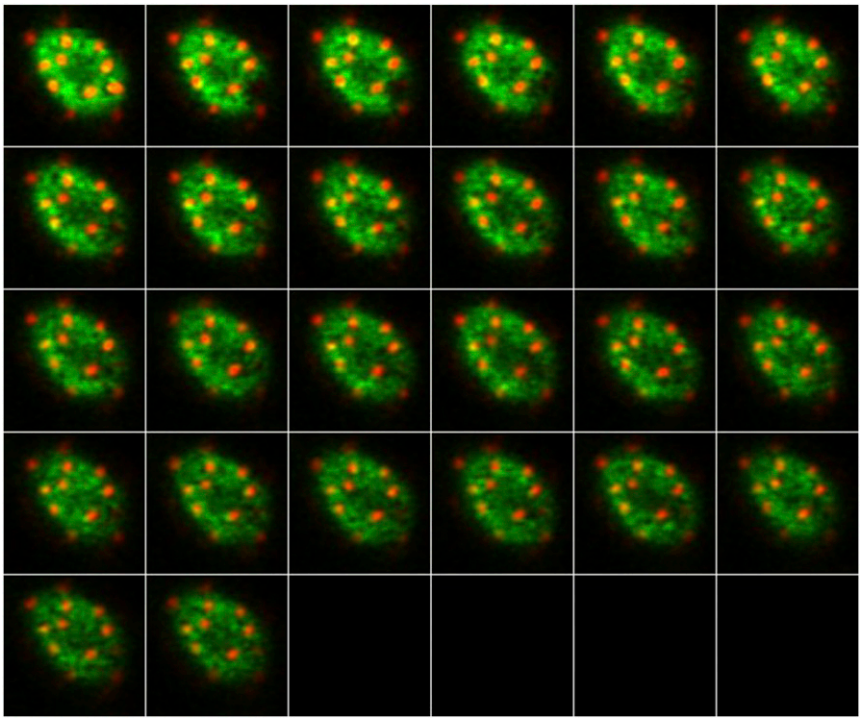

Movie S2. Representative FRAP analysis of Can1(7KR)-GFP in the EMC in the presence of substrate. Frames correspond to 20-s intervals, up to 480 s after photobleaching. Related to Fig. 1*C*.

Movie S2

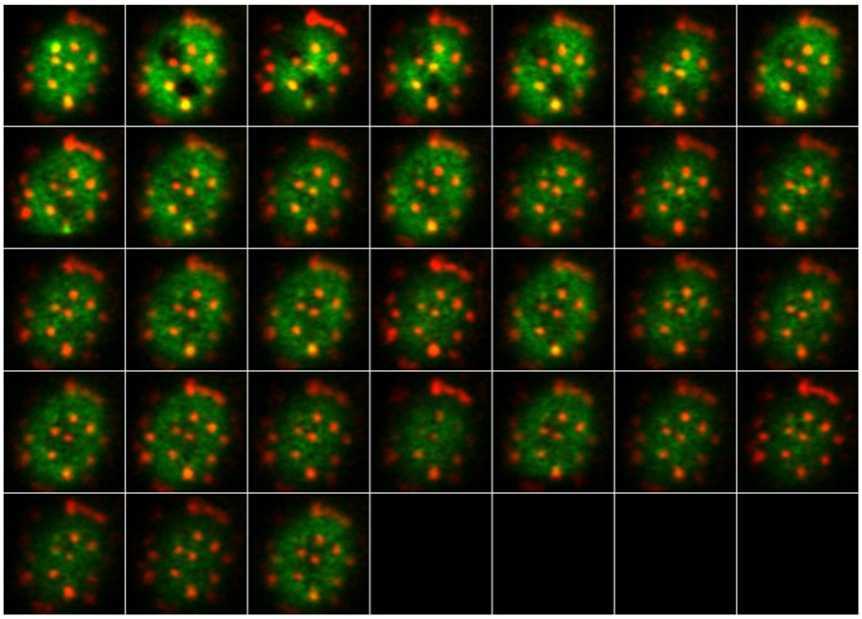

Movie S3. Representative FRAP analysis of Can1(7KR)-GFP outside the EMC, in the absence of substrate. Frames correspond to 20-s intervals, up to 580 s after photobleaching. Related to Fig. 1*C*.

Movie S3

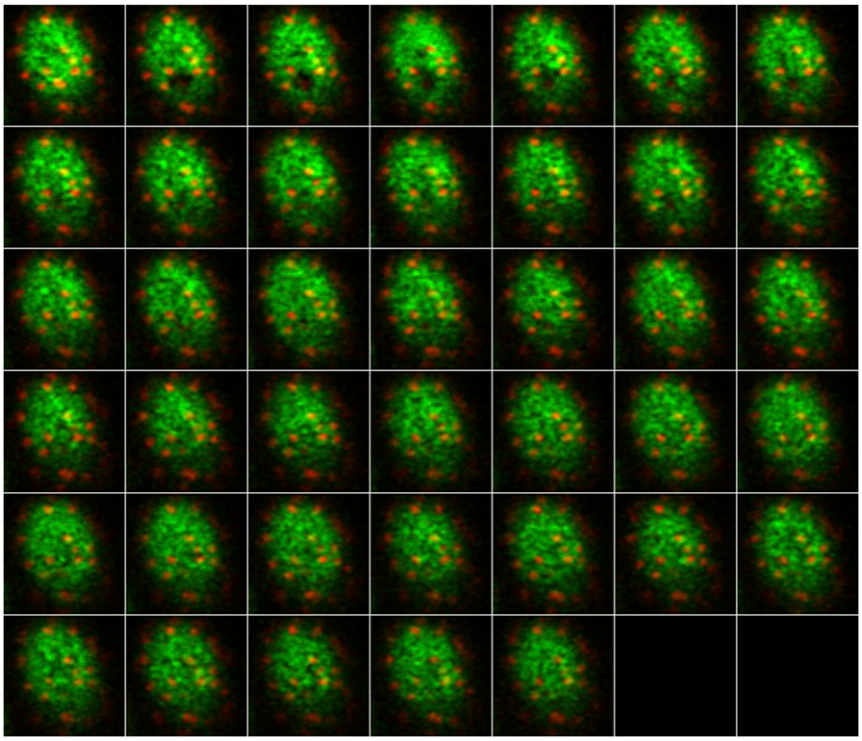

Movie S4. Representative FRAP analysis of Can1(E184Q)-GFP. Frames correspond to 10-s intervals, up to 380 s after photobleaching. Related to Fig. 2*D*.

Movie S4

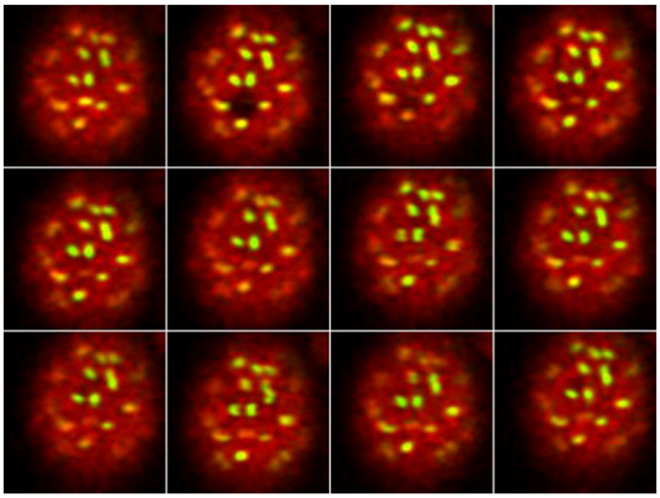

Movie S5. Representative FRAP analysis of Can1(7KR)-mCherry in Pil1(4A)-GFP–containing EMCs. Frames correspond to 2-min intervals, up to 20 min after photobleaching. Related to Fig. 3C.

Movie S5

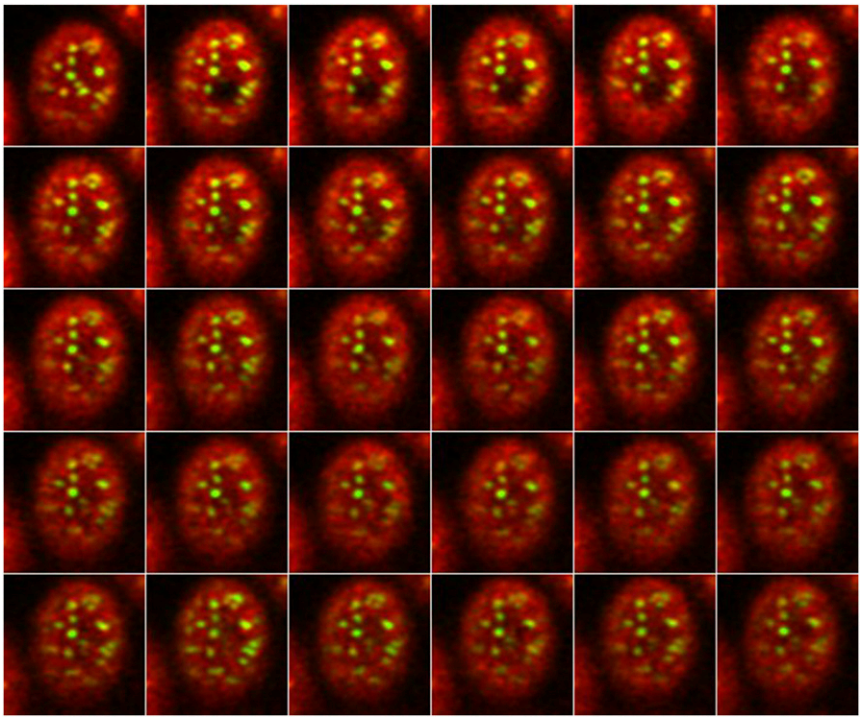

Movie S6. Representative FRAP analysis of Can1(7KR)-mCherry in Pil1(4A)-GFP–containing EMCs in cells treated with 10 μM Myr for 90 min. Frames correspond to 20-s intervals, up to 560 s after photobleaching. Related to Fig. 3C.

Movie S6

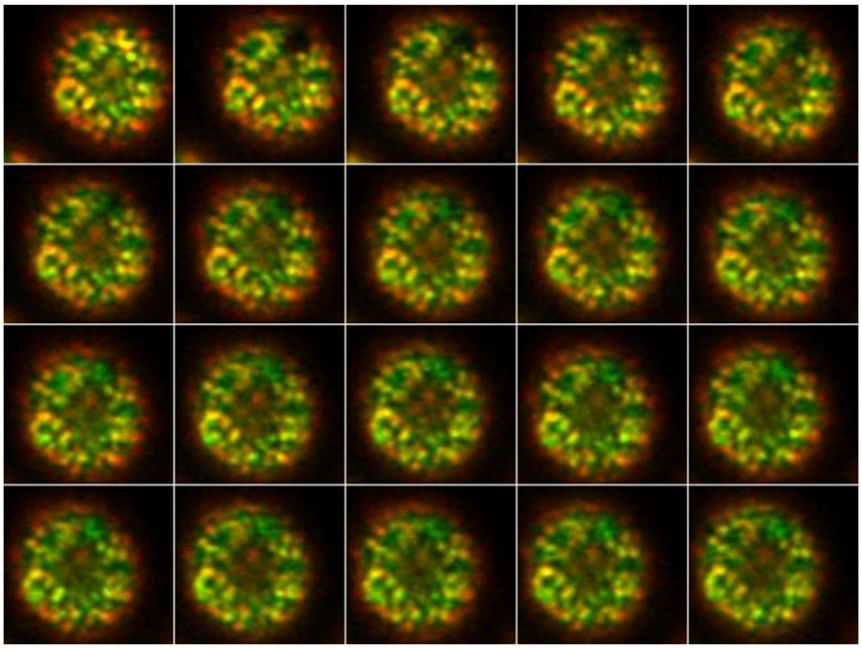

Movie S7. Representative FRAP analysis of Can1(7KR)-GFP in the EMC in the late stationary phase. Frames correspond to 2-min intervals, up to 36 min after photobleaching. Related to Fig. 5*G*.

Movie S7